

January 2011

## Chemically activated reactions on the C<sub>7</sub>H<sub>5</sub> energy surface: Propargyl + diacetylene, i-C<sub>5</sub>H<sub>3</sub> + acetylene, and n-C<sub>5</sub>H<sub>3</sub> + acetylene

Gabriel da Silva

Adam J. Trevitt

*University of Wollongong*, adamt@uow.edu.au

Follow this and additional works at: <https://ro.uow.edu.au/scipapers>



Part of the [Life Sciences Commons](#), [Physical Sciences and Mathematics Commons](#), and the [Social and Behavioral Sciences Commons](#)

---

### Recommended Citation

da Silva, Gabriel and Trevitt, Adam J.: Chemically activated reactions on the C<sub>7</sub>H<sub>5</sub> energy surface: Propargyl + diacetylene, i-C<sub>5</sub>H<sub>3</sub> + acetylene, and n-C<sub>5</sub>H<sub>3</sub> + acetylene 2011, 8940-8952.  
<https://ro.uow.edu.au/scipapers/1022>

---

# Chemically activated reactions on the C<sub>7</sub>H<sub>5</sub> energy surface: Propargyl + diacetylene, i-C<sub>5</sub>H<sub>3</sub> + acetylene, and n-C<sub>5</sub>H<sub>3</sub> + acetylene

## Abstract

This study uses computational chemistry and statistical reaction rate theory to investigate the chemically activated reaction of diacetylene (butadiyne, C<sub>4</sub>H<sub>2</sub>) with the propargyl radical (C<sub>3</sub>H<sub>3</sub>) and the reaction of acetylene (C<sub>2</sub>H<sub>2</sub>) with the i-C<sub>5</sub>H<sub>3</sub> (CH<sub>2</sub>CCCC•H) and n-C<sub>5</sub>H<sub>3</sub> (CHCC•HCCH) radicals. A detailed G3SX-level C<sub>7</sub>H<sub>5</sub> energy surface demonstrates that the C<sub>3</sub>H<sub>3</sub> + C<sub>4</sub>H<sub>2</sub> and C<sub>5</sub>H<sub>3</sub> + C<sub>2</sub>H<sub>2</sub> addition reactions proceed with moderate barriers, on the order of 10 to 15 kcal mol<sup>-1</sup>, and form activated open-chain C<sub>7</sub>H<sub>5</sub> species that can isomerize to the fulvenallenyl radical with the highest barrier still significantly below the entrance channel energy. Higher-energy pathways are available leading to other C<sub>7</sub>H<sub>5</sub> isomers and to a number of C<sub>7</sub>H<sub>4</sub> species + H. Rate constants in the large multiple-well (15) multiple-channel (30) chemically activated system are obtained from a stochastic solution of the one-dimensional master equation, with RRKM theory for microcanonical rate constants. The dominant products of the C<sub>4</sub>H<sub>2</sub> + C<sub>3</sub>H<sub>3</sub> reaction at combustion-relevant temperatures and pressures are i-C<sub>5</sub>H<sub>3</sub> + C<sub>2</sub>H<sub>2</sub> and CH<sub>2</sub>CCHCCCCH + H, along with several quenched C<sub>7</sub>H<sub>5</sub> intermediate species below 1500 K. The major products in the n-C<sub>5</sub>H<sub>3</sub> + C<sub>2</sub>H<sub>2</sub> reaction are i-C<sub>5</sub>H<sub>3</sub> + C<sub>2</sub>H<sub>2</sub> and a number of C<sub>7</sub>H<sub>4</sub> species + H, with C<sub>7</sub>H<sub>5</sub> radical stabilization at lower temperatures. The i-C<sub>5</sub>H<sub>3</sub> + C<sub>2</sub>H<sub>2</sub> reaction predominantly leads to C<sub>7</sub>H<sub>4</sub> + H and to stabilized C<sub>7</sub>H<sub>5</sub> products. The title reactions may play an important role in polycyclic aromatic hydrocarbon (PAH) formation in combustion systems. The C<sub>7</sub>H<sub>5</sub> potential energy surface developed here also provides insight into several other important reacting gas-phase systems relevant to combustion and astrochemistry, including C<sub>2</sub>H + the C<sub>3</sub>H<sub>4</sub> isomers propyne and allene, benzyne + CH, benzene + C(3P), and C<sub>7</sub>H<sub>5</sub> radical decomposition, for which some preliminary analysis is presented. © 2011 the Owner Societies.

## Keywords

diacetylene, propargyl, surface, energy, c<sub>7</sub>h<sub>5</sub>, reactions, n, activated, acetylene, chemically, c<sub>5</sub>h<sub>3</sub>, i, GeoQUEST

## Disciplines

Life Sciences | Physical Sciences and Mathematics | Social and Behavioral Sciences

## Publication Details

da Silva, G. & Trevitt, A. J. (2011). Chemically activated reactions on the C<sub>7</sub>H<sub>5</sub> energy surface: Propargyl + diacetylene, i-C<sub>5</sub>H<sub>3</sub> + acetylene, and n-C<sub>5</sub>H<sub>3</sub> + acetylene. *Physical Chemistry Chemical Physics*, 13 (19), 8940-8952.

Cite this: *Phys. Chem. Chem. Phys.*, 2011, **13**, 8940–8952

www.rsc.org/pccp

PAPER

# Chemically activated reactions on the $C_7H_5$ energy surface: propargyl + diacetylene, $i-C_5H_3$ + acetylene, and $n-C_5H_3$ + acetylene†

Gabriel da Silva\*<sup>a</sup> and Adam J. Trevitt<sup>b</sup>

Received 13th January 2011, Accepted 8th March 2011

DOI: 10.1039/c1cp20112c

This study uses computational chemistry and statistical reaction rate theory to investigate the chemically activated reaction of diacetylene (butadiyne,  $C_4H_2$ ) with the propargyl radical ( $C^{\bullet}H_2CCH$ ) and the reaction of acetylene ( $C_2H_2$ ) with the  $i-C_5H_3$  ( $CH_2CCCC^{\bullet}H$ ) and  $n-C_5H_3$  ( $CHCC^{\bullet}HCCH$ ) radicals. A detailed G3SX-level  $C_7H_5$  energy surface demonstrates that the  $C_3H_3 + C_4H_2$  and  $C_5H_3 + C_2H_2$  addition reactions proceed with moderate barriers, on the order of 10 to 15 kcal mol<sup>-1</sup>, and form activated open-chain  $C_7H_5$  species that can isomerize to the fulvenallenyl radical with the highest barrier still significantly below the entrance channel energy. Higher-energy pathways are available leading to other  $C_7H_5$  isomers and to a number of  $C_7H_4$  species + H. Rate constants in the large multiple-well (15) multiple-channel (30) chemically activated system are obtained from a stochastic solution of the one-dimensional master equation, with RRKM theory for microcanonical rate constants. The dominant products of the  $C_4H_2 + C_3H_3$  reaction at combustion-relevant temperatures and pressures are  $i-C_5H_3 + C_2H_2$  and  $CH_2CCHCCCH + H$ , along with several quenched  $C_7H_5$  intermediate species below 1500 K. The major products in the  $n-C_5H_3 + C_2H_2$  reaction are  $i-C_5H_3 + C_2H_2$  and a number of  $C_7H_4$  species + H, with  $C_7H_5$  radical stabilization at lower temperatures. The  $i-C_5H_3 + C_2H_2$  reaction predominantly leads to  $C_7H_4 + H$  and to stabilized  $C_7H_5$  products. The title reactions may play an important role in polycyclic aromatic hydrocarbon (PAH) formation in combustion systems. The  $C_7H_5$  potential energy surface developed here also provides insight into several other important reacting gas-phase systems relevant to combustion and astrochemistry, including  $C_2H +$  the  $C_3H_4$  isomers propyne and allene, benzyne + CH, benzene +  $C(^3P)$ , and  $C_7H_5$  radical decomposition, for which some preliminary analysis is presented.

## Introduction

Polyynes, consisting of multiple acetylene  $-C\equiv C-$  units, are encountered in a variety of reacting gas-phase systems. They are known to occur in the interstellar medium (ISM)<sup>1</sup> and in flames,<sup>2,3</sup> and may also play a role in the atmospheric chemistry of Saturn's moon Titan.<sup>4</sup> Common among these disparate environments is the presence of polycyclic aromatic hydrocarbons (PAHs). PAHs account for most of the carbon present in deep space, contribute to Titan's hydrocarbon haze, and are a major pollutant and health concern here on Earth.

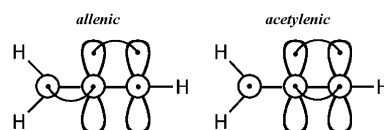
<sup>a</sup> Chemical and Biomolecular Engineering, The University of Melbourne, Victoria 3010, Australia. E-mail: gdasilva@unimelb.edu.au

<sup>b</sup> School of Chemistry, University of Wollongong, New South Wales 2522, Australia

† Electronic Supplementary Information (ESI) available: Structures for  $C_7H_5$  and  $C_7H_4$  species and transition states; Cartesian coordinates, vibrational frequencies, and moments of inertia for optimized species; G3SX energies; thermochemical properties; internal rotor potentials; canonical rate constants; calculated rate constants,  $k(T,P)$ ; and complete  $C_7H_5$  energy surface.

The role played by polyynes in the chemistry of PAH formation is not well understood.

The reaction of polyynes with resonantly stabilized free radicals is one possible mechanism for PAH formation. A potentially important candidate implicated in this chemistry is the propargyl radical ( $C_3H_3$ ), which is stabilized by resonance between the allenic ( $CH_2=C=C^{\bullet}H$ ) and acetylenic ( $H_2C^{\bullet}-C\equiv CH$ ) forms (Scheme 1). Like polyne molecules, propargyl is formed in sooting flames, while it is also predicted to play an important role in aromatic hydrocarbon formation on Titan. The reaction of diacetylene and other polyynes with propargyl has the potential to contribute to PAH formation in



**Scheme 1** General valence bond (GVB) diagrams for the allenic and acetylenic resonance structures of the propargyl radical.

a variety of environments, yet these reaction classes have not been explored in detail. Indarto *et al.*<sup>5</sup> recently examined the possibility of diacetylene reacting with propargyl (as well as other free radicals) to form cyclic compounds with some triradical character. This so-called radical breeding mechanism<sup>6</sup> was found to be unfavored in terms of free energy for  $C_4H_2 + C_3H_3$ . Alternative pathways are however available to  $C_7H_5$  products with a single radical center; to date these pathways have not been investigated.

This study is principally concerned with the mechanism and kinetics of the chemically activated reaction of diacetylene with the propargyl radical. A low-energy pathway is found that connects these reactants with the  $C_7H_5$  fulvenallenyl radical, a resonantly stabilized free radical that has been recently proposed as a PAH pre-cursor.<sup>7</sup> Subsequent addition of  $C_4H_2$  to the fulvenallenyl radical can enlarge this species *via* one benzene ring, following a similar mechanism to the propargyl + diacetylene reaction. The  $C_3H_3 + nC_4H_2$  process is a plausible new mechanism capable of initiating and then propagating PAH growth. The  $C_7H_5$  energy surface developed in this study also provides us with an opportunity to study the reaction of two common  $C_5H_3$  radicals with acetylene, which may also be involved in PAH formation.

## Computational methods

### Electronic structure theory calculations

All species reported here are studied using the G3SX composite theoretical methodology.<sup>8</sup> This method uses B3LYP/6-31G(2df,p) optimized geometries, vibrational frequencies and scaled zero point energies, with higher-level wavefunction theory calculations for accurate energies (along with empirical scaling corrections). Compared to computational methods of similar cost, the G3SX method provides excellent accuracy, particularly with respect to barrier heights.<sup>8,9</sup> Reported G3SX energies (barrier heights, reaction enthalpies, and heats of formation) are expected to have mean uncertainties of around 0.4 to 0.8 kcal mol<sup>-1</sup>,<sup>8-10</sup> with 95% uncertainty intervals conservatively placed at  $\pm 1.5$  kcal mol<sup>-1</sup>. Electronic structure calculations are carried out in Gaussian 09.<sup>11</sup> Cartesian coordinates, G3SX energies, and vibrational frequencies for all reported stationary points are provided as ESI.†

Enthalpies of formation ( $\Delta_f H^\circ_0$ , kcal mol<sup>-1</sup>) are determined for all minima and transition states from 0 K G3SX energies, using an atomization methodology. This procedure, in conjunction with the G3SX method, has been shown to produce heats of formation of similar accuracy to isodesmic calculations (mean unsigned error of 0.33 kcal mol<sup>-1</sup> for a series of closed-shell hydrocarbons).<sup>10</sup> Additionally, adiabatic ionization energies (AIEs) and vertical ionization energies (VIEs) are determined for  $C_7H_5$  radicals (including several previously-considered isomers otherwise not involved in this study). Ionization energies are from 0 K G3SX energies, with VIEs obtained using frozen  $C_7H_5$  radical structures in the  $C_7H_5^+$  ion energy determinations (whereas AIEs use the  $C_7H_5$  radical structures as the starting point for calculating re-optimized  $C_7H_5^+$  geometries).

### Thermochemistry and kinetics calculations

The MultiWell-2010.1 suite of programs is used to perform all thermochemistry, canonical transition state theory, and statistical reaction rate theory (RRKM/ME) calculations.<sup>12</sup>

Entropy ( $S^\circ_{298}$ ) and heat capacity ( $C_p$ , 300–2000 K) values in cal mol<sup>-1</sup> K<sup>-1</sup> units are reported for all species, in addition to 0 K and 298 K heats of formation (in the ESI.†). These properties are calculated according to standard principles of statistical mechanics, using B3LYP/6-31G(2df,p) structural parameters and vibrational frequencies. Corrections for external molecular symmetry and optical isomers are also included as appropriate.

Low-energy torsional modes of the open-chain  $C_7H_5$  isomers, and of the corresponding transition states for C–C dissociation, are treated as unsymmetrical one-dimensional hindered internal rotations. This treatment is required to accurately describe the entropy change upon cyclization. Relaxed geometry dihedral angle scans at the B3LYP/6-31G(2df,p) level are used to obtain potential energies and corresponding Cartesian coordinates as a function of dihedral angle, in 5° intervals (with the cleaving C–C bond frozen in the transition states). The lamm program within the MultiWell suite is then used to determine torsion rotational constants for each structure through 360°. Rotational constants and rotor potentials are fit to eight-parameter truncated Fourier series expansions, providing the constants required to replace the corresponding harmonic oscillator vibrational frequency in the partition function calculations. Rotor potentials are illustrated in the ESI.†

For elementary reactions, rate constants in the high-pressure limit are obtained from the reported thermochemical properties of the reactants, products, and transition states *via* canonical transition state theory. High-pressure limit rate constants for the bimolecular  $C_4H_2 + C_3H_3$  and  $C_5H_3 + C_2H_2$  reactions are required to calculate apparent rate constants to different product sets in the chemically activated systems, whereas rate constants for other reactions are reported for the sake of posterity. Rate constants obtained between 300 and 2000 K are fit to the three-parameter form of the Arrhenius equation, yielding the constants  $A'$ ,  $n$ , and  $E_a$ . All reported rate constants ( $k$ ) and pre-exponential factors ( $A'T^n$ ) are in units of cm<sup>3</sup> molecule<sup>-1</sup> s<sup>-1</sup> (second order) and s<sup>-1</sup> (first order), with  $E_a$  in kcal mol<sup>-1</sup> and temperature ( $T$ ) in K.

Branching ratios to product sets in chemically activated reactions on the  $C_7H_5$  energy surface, comprising a large multiple-well (15) multiple-reaction-channel (30) system, are determined by solving the one-dimensional master equation using a stochastic method. Densities and sums of states are determined from Stein–Rabinovitch–Beyer–Swinehart counts, based upon molecular properties identical to those used in the thermochemistry calculations described above. RRKM theory is used to calculate microcanonical energy-dependent unimolecular rate constants,  $k(E)$ . Wells are assumed to be symmetric (oblate or prolate) tops, with external rotation described using an inactive 2D and an active 1D rotor. Conservation of angular momentum is achieved by way of a centrifugal correction (for reactions that do not involve tunneling).

For intramolecular hydrogen shift reactions, transition state sums of states, and thus microcanonical rate constants, are corrected for quantum mechanical tunneling (note that the canonical high-pressure limit rate constants also reported in this study are not adjusted for tunneling). The curvature of the potential energy surface along the reaction coordinate in the vicinity of a transition state is described by that transition state's imaginary vibrational frequency, with tunneling corrections computed according to a one-dimensional unsymmetrical Eckart barrier. No tunneling corrections are applied to H atom dissociation reactions, where the critical reaction energy is similar to the enthalpy of reaction (*i.e.*, the intrinsic component of the barrier is small).

MultiWell implements a hybrid formulation of the master equation, with an energy-grained master equation at low energies and a continuum master equation at high energies. At low energies, an energy grain of  $10\text{ cm}^{-1}$  is employed, with properties evaluated up to a maximum energy of  $9990\text{ cm}^{-1}$  (*i.e.*, across 1000 grains). The continuum master equation is then solved up to a maximum energy of  $150\,000\text{ cm}^{-1}$  over a further 1000 grains. Collisional energy transfer is treated using an exponential-down model with a constant  $\Delta E_{\text{down}}$  value of  $1000\text{ cm}^{-1}$  and Lennard-Jones parameters of  $\sigma = 5.9\text{ \AA}$  and  $\varepsilon/k_{\text{B}} = 410\text{ K}$  for the active  $\text{C}_7\text{H}_5$  isomers. The buffer gas is  $\text{N}_2$ .

For all reported simulations, one million trials were conducted for 200 collisions each, at temperatures between 100 and 2000 K and pressures between 0.001 and 100 atm. Yields of all reported products were found to have converged within 200 collisions, or to have reached a quasi-steady value before decaying due to further thermal unimolecular reaction (or conversely, growing due to flux in from one of these thermal reaction channels) upon reaching what is essentially a Boltzmann energy distribution. In the latter case, yields were determined at a time when negligible thermal isomerization/dissociation was deemed to have occurred, which was seen to essentially obey the rate constant expressions determined from canonical transition state theory (keeping fall-off effects in mind), from natural log plots of yield *versus* time. Apparent rate constants,  $k(T, P)$ , for the formation of important

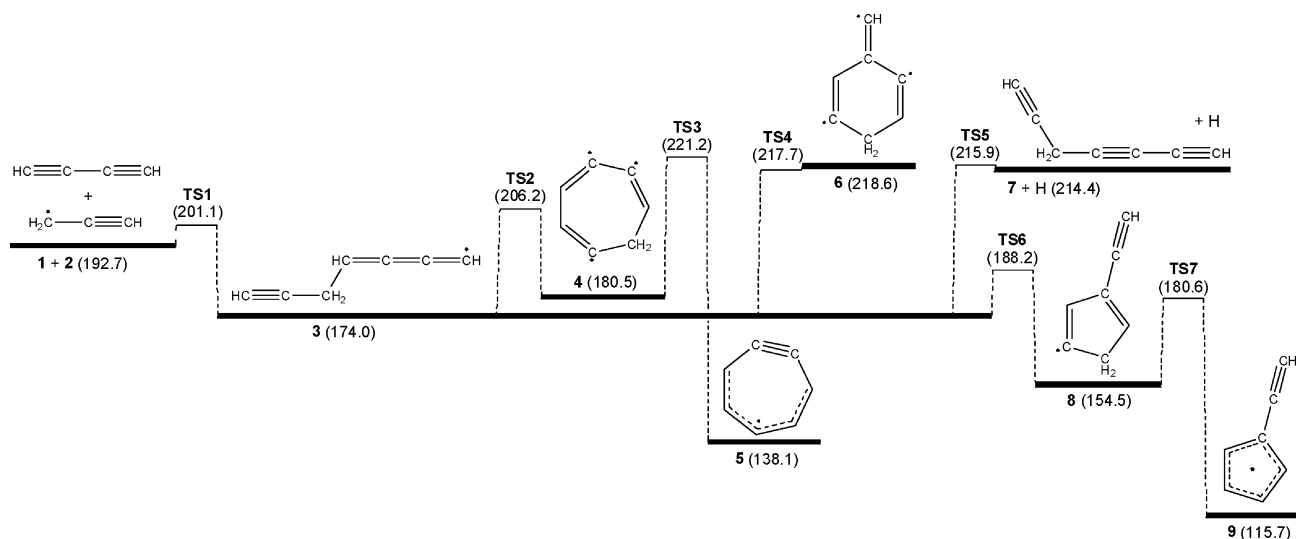
products in chemically activated reactions were determined from product yields and bimolecular reaction rate constants. These rate constants are reported in the form  $k = A'T''\exp(-E_a/RT)$  to facilitate inclusion in detailed kinetic models, and individual  $k(T, P)$  values are also provided in the ESI.†

## Results and discussion

### $\text{C}_7\text{H}_5$ energy surface

This study investigates the association of a terminal C atom in  $\text{C}_4\text{H}_2$  with the propargyl radical to form both acetylenic and allenic adducts (*cf.* Scheme 1). The sub-section of the  $\text{C}_7\text{H}_5$  energy surface representing initial formation of the acetylenic adduct is shown in Fig. 1, whereas the energy surface representing formation of the allenic adduct is depicted in Fig. 2. In both cases bimolecular reaction initially proceeds *via* an adiabatic transition state; for formation of the acetylenic adduct the barrier height is  $8.4\text{ kcal mol}^{-1}$ , while for formation of the allenic adduct it is  $10.7\text{ kcal mol}^{-1}$ . The  $\text{C}_7\text{H}_5$  product in both mechanisms is around  $20\text{ kcal mol}^{-1}$  more stable than the reactants, or around  $30\text{ kcal mol}^{-1}$  below the energy of the entrance channel transition state. In the chemically activated  $\text{C}_3\text{H}_3 + \text{C}_4\text{H}_2$  reaction these  $\text{C}_7\text{H}_5$  radicals are therefore provided with a reasonable degree of excess vibrational energy that can be utilized in further isomerization and dissociation processes.

The chemically activated acetylenic adduct (**3**) formed from  $\text{C}_4\text{H}_2$  association with propargyl depicted in Fig. 1 has cyclization channels available to five-, six-, and seven-member ring compounds. Pathways to the seven-member (**4**) and six-member (**6**) triradicals were reported in ref. 5, and both reactions must surmount barriers above the entrance channel energy (although formation of a seven-member ring compound *via* **TS2** occurs just above the entrance channel energy). The six-member ring triradical is close to being unstable, and will not be of any significance. The seven-member ring compound, however, has an appreciable barrier for reverse



**Fig. 1** Energy surface for  $\text{C}_4\text{H}_2$  addition to  $\text{C}_3\text{H}_3$  to form an acetylenic adduct (G3SX enthalpies of formation,  $\text{kcal mol}^{-1}$ ).

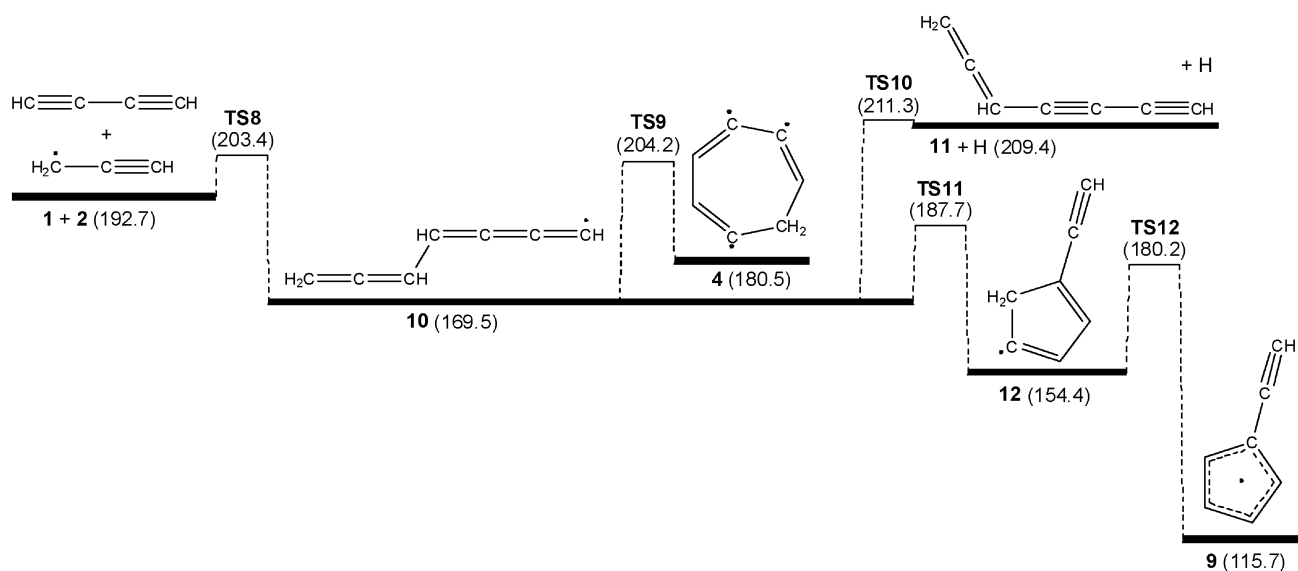


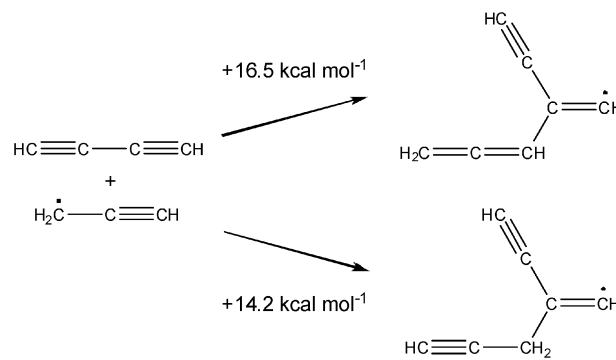
Fig. 2 Energy surface for C<sub>4</sub>H<sub>2</sub> addition to C<sub>3</sub>H<sub>3</sub> to form an allenic adduct (G3SX enthalpies of formation, kcal mol<sup>-1</sup>).

reaction, and may be able to undergo collisional deactivation or further isomerization in the chemically activated C<sub>4</sub>H<sub>2</sub> + C<sub>3</sub>H<sub>3</sub> reaction. The energy surface reported here illustrates how this C<sub>7</sub>H<sub>5</sub> compound can undergo an intramolecular hydrogen shift to produce the *c*-C<sub>7</sub>H<sub>5</sub> radical **5**, which has been previously considered as a product of the benzene + C(<sup>3</sup>P) reaction.<sup>13</sup> While this *c*-C<sub>7</sub>H<sub>5</sub> radical is considerably more stable than the open-chain isomer **3**, the tight transition state for intramolecular H atom migration results in a considerably larger barrier for forward reaction of **4** than for the reverse isomerization back to **3**. The seven-membered ring radical **4** can also transfer a H atom across the ring, in a 1,4-hydrogen shift similar to that which Cavallotti and co-workers have identified as being important in C<sub>7</sub>H<sub>7</sub> radical chemistry,<sup>14</sup> although the large barrier height, 45.4 kcal mol<sup>-1</sup> above ground state C<sub>4</sub>H<sub>2</sub> + C<sub>3</sub>H<sub>3</sub>, will make this insignificant and it is not considered further. The open-chain C<sub>7</sub>H<sub>5</sub> isomer **3** can also undergo C–H bond homolysis to give the C<sub>7</sub>H<sub>4</sub> species HC≡CCH<sub>2</sub>C≡CC≡CH (1,3,6-heptatriyne, **7**) + H, with a barrier of 14.8 kcal mol<sup>-1</sup> above the entrance channel energy. While this process is expected to be of minimal importance at low to moderate temperatures, it may play a role at high temperatures.

By far, the lowest energy pathway identified for isomerization of **3** is to the five-membered ring compound **8**. This is a radical propagating process, and was subsequently not considered in the radical breeding study of Indarto *et al.*<sup>5</sup> The barrier for isomerization of **3** to **8** falls 12.9 kcal mol<sup>-1</sup> below the entrance channel transition state in this chemically activated C<sub>3</sub>H<sub>3</sub> + C<sub>4</sub>H<sub>2</sub> process. The five-membered ring-closing product (**8**) can isomerize to the fulvenallenyl radical (**9**) via a 1,2-hydrogen shift, with a small barrier. The fulvenallenyl radical has a large degree of resonance stabilization,<sup>7</sup> due to the presence of propargyl- and cyclopentadienyl-like radical forms. Accordingly, isomerization of **8** to **9** is considerably exothermic (38.8 kcal mol<sup>-1</sup>) and the reverse reaction back to C<sub>3</sub>H<sub>3</sub> + C<sub>4</sub>H<sub>2</sub> is faced with a large barrier (85.4 kcal mol<sup>-1</sup>).

Addition of C<sub>4</sub>H<sub>2</sub> to propargyl to form the allenic adduct **10**, which is depicted in Fig. 2, requires a larger barrier than the corresponding process for the acetylenic adduct. This provides **10** with slightly more excess vibrational energy than **3**, but also means that it will be formed at a slower rate. The further reaction pathways available to **10** are analogous to those of **3**, except that no transition states were located to six-membered ring compounds. This is not entirely surprising, given the negligible energy required for ring-opening of the six-membered ring species **6** depicted in Fig. 1. The C<sub>7</sub>H<sub>5</sub> isomer **10** can undergo radical-breeding isomerization to **4**, the seven-membered ring produced in the alternate C<sub>3</sub>H<sub>3</sub> + C<sub>4</sub>H<sub>2</sub> process. Again, this reaction proceeds at around the same energy as the entrance channel. The cyclization reaction of **10** to the five-membered ring compound **12** requires a barrier of only 18.2 kcal mol<sup>-1</sup>, which places it 15.7 kcal mol<sup>-1</sup> below the entrance channel energy. Again, a facile 1,2-hydrogen shift produces the fulvenallenyl radical. Finally, C–H dissociation in **10** can also occur, producing CH<sub>2</sub>=C=CHC≡CC≡CH (1,2-heptadiene-4,6-diyne, **11**) + H. This reaction proceeds at 7.9 kcal mol<sup>-1</sup> above the entrance channel energy (18.6 kcal mol<sup>-1</sup> above the reactants).

In addition to the processes considered above, the propargyl radical can add to a secondary C atom in diacetylene, as shown below. These reactions encounter barriers larger than



14 kcal mol<sup>-1</sup> and are unlikely to be of much significance compared to the processes revealed in Fig. 1 and 2; as such they are not explored any further.

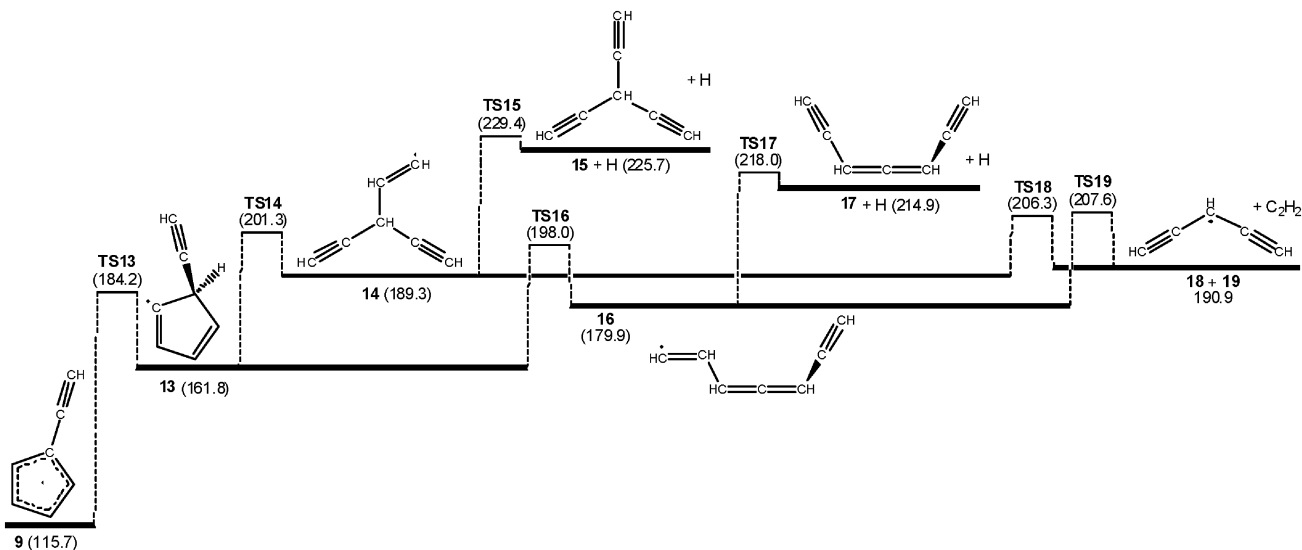
In the master equation simulations reported here, the full energy surface for the C<sub>4</sub>H<sub>2</sub> + C<sub>3</sub>H<sub>3</sub> reaction features the pathways identified in Fig. 1 and 2 for both the acetylenic and allenic addition processes (excluding formation of **6**); this complete energy surface is depicted in the ESI.† This allows for isomerization of fulvenallenyl *via* both **8** and **12**, irrespective of the initial C<sub>7</sub>H<sub>5</sub> isomer formed, which is important in describing fulvenallenyl radical decomposition at high temperatures. It is also important to consider possible C<sub>7</sub>H<sub>5</sub> radical decomposition channels to acetylene plus a C<sub>5</sub>H<sub>3</sub> radical at higher temperatures. It is well accepted that the two most stable C<sub>5</sub>H<sub>3</sub> radicals are the *i*-C<sub>5</sub>H<sub>3</sub> (CH<sub>2</sub>CCCCH) and *n*-C<sub>5</sub>H<sub>3</sub> (CHCCHCCH) isomers,<sup>15</sup> and reaction pathways to these two product channels are also included in our full C<sub>4</sub>H<sub>2</sub> + C<sub>3</sub>H<sub>3</sub> potential energy surface. Furthermore, this energy surface is also used to study the kinetics of these two important C<sub>5</sub>H<sub>3</sub> radicals reacting with acetylene.

Pathways to the *n*-C<sub>5</sub>H<sub>3</sub> radical (**18**) + C<sub>2</sub>H<sub>2</sub> (**19**) from the fulvenallenyl radical are depicted in Fig. 3. We observe that this product set is similar to C<sub>4</sub>H<sub>2</sub> + C<sub>3</sub>H<sub>3</sub> in energy, while the requisite barrier heights are also located at around the energy of the C<sub>4</sub>H<sub>2</sub> + C<sub>3</sub>H<sub>3</sub> entrance channels. The elementary reaction steps depicted in Fig. 3 again involve an intramolecular

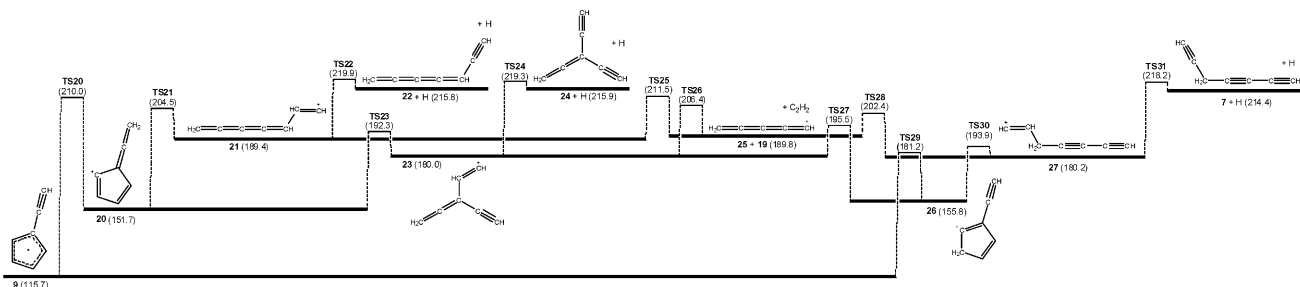
H atom shift in the fulvenallenyl radical (to **13**), followed by ring opening to either **14** or **16**. These open-chain C<sub>7</sub>H<sub>5</sub> isomers can either dissociate to *n*-C<sub>5</sub>H<sub>3</sub> + C<sub>2</sub>H<sub>2</sub>, or lose a H atom to produce a C<sub>7</sub>H<sub>4</sub> polyne.

The mechanism developed for *i*-C<sub>5</sub>H<sub>3</sub> + C<sub>2</sub>H<sub>2</sub> formation in the C<sub>4</sub>H<sub>2</sub> + C<sub>3</sub>H<sub>3</sub> reaction is shown in Fig. 4. The *i*-C<sub>5</sub>H<sub>3</sub> radical is predicted to be around 1 kcal mol<sup>-1</sup> more stable than the *n*-C<sub>5</sub>H<sub>3</sub> form, while barrier heights for association of C<sub>2</sub>H<sub>2</sub> at the three available radical sites are in the range of 12.6–21.7 kcal mol<sup>-1</sup>. In Fig. 4 we observe that H atom migrations in the fulvenallenyl radical can lead to the production of two different *i*-C<sub>5</sub>H<sub>3</sub> pre-cursors, **20** and **26**, where the barrier to form **20** is considerably larger than that of any other considered H-shift in **9**. The five-member ring compound **20** can participate in ring-opening reactions to **21** and **23**, while **26** can undergo similar reactions to **23** and **27**. As well as dissociating to *i*-C<sub>5</sub>H<sub>3</sub> + C<sub>2</sub>H<sub>2</sub>, each of the three open-chain C<sub>7</sub>H<sub>5</sub> radicals can undergo C–H bond dissociation to form a highly unsaturated C<sub>7</sub>H<sub>4</sub> species (**7**, **22**, **24**) + H, with barriers again considerably above the entrance channel energy.

The complete C<sub>7</sub>H<sub>5</sub> energy surface developed here (depicted in the ESI†) comprises a 15 well, 30 reaction-channel system, and is utilized in the following sections to study the C<sub>4</sub>H<sub>2</sub> + C<sub>3</sub>H<sub>3</sub> reaction, as well as the *i*-C<sub>5</sub>H<sub>3</sub>/*n*-C<sub>5</sub>H<sub>3</sub> + C<sub>2</sub>H<sub>2</sub> processes. All optimized C<sub>7</sub>H<sub>5</sub> and C<sub>7</sub>H<sub>4</sub> minima involved in the proposed C<sub>7</sub>H<sub>5</sub> potential energy surface are shown in the



**Fig. 3** Energy surface for the fulvenallenyl radical (**9**) decomposition to the *n*-C<sub>5</sub>H<sub>3</sub> radical (**18**) + C<sub>2</sub>H<sub>2</sub> (G3SX enthalpies of formation, kcal mol<sup>-1</sup>).



**Fig. 4** Energy surface for the fulvenallenyl radical (**9**) decomposition to the *i*-C<sub>5</sub>H<sub>3</sub> radical (**25**) + C<sub>2</sub>H<sub>2</sub> (G3SX enthalpies of formation, kcal mol<sup>-1</sup>).

ESI,<sup>†</sup> along with transition state structures. Thermochemical properties ( $\Delta_f H^\circ_0$ ,  $\Delta_f H^\circ_{298}$ ,  $S^\circ_{298}$ ,  $C_p(T)$ ) for all species and rate constant parameters for all elementary reactions are also provided.

### $C_4H_2 + C_3H_3$ reaction kinetics

Rate constants to different products in the proposed  $C_4H_2 + C_3H_3$  reaction mechanism have been determined as a function of temperature and pressure from RRKM/ME calculations. Simulations were executed separately for the two addition mechanisms, with total rate constants then obtained by summing the two processes. The only important reaction products, defined as accounting for at least 1% of new product formation at some studied temperature and pressure, are **3**, **8**, **9**, **10**, **13**, **20**, **26**, **7 + H**, **11 + H**, **18 + 19**, and **25 + 19**, along with the reverse reaction to  $C_4H_2 + C_3H_3$ . Calculated rate constants to these products are listed in the ESI,<sup>†</sup> with rate constant parameters  $E_a$ ,  $A'$ , and  $n$  provided in Table 1 for 10 atm and in the ESI<sup>†</sup> for other pressures.

Due to the appreciable association barrier, the  $C_4H_2 + C_3H_3$  reaction is expected to be significantly operative only at combustion-relevant temperatures. This barrier renders the

**Table 1** Rate constant parameters for the formation of important products in the  $C_3H_3 + C_4H_2$  reaction, at 10 atm between 300 and 2000 K<sup>a</sup>

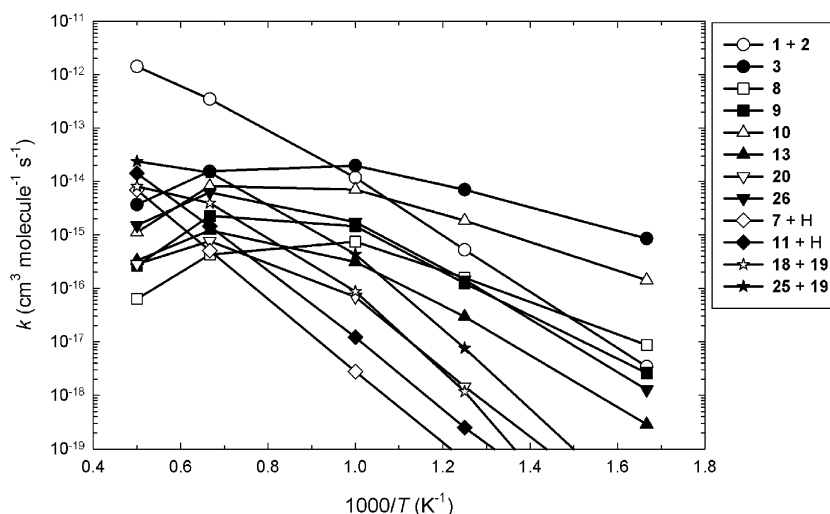
	$E_a$	$A'$	$n$
<b>1 + 2 → 3</b>	15.40	$3.48 \times 10^7$	-6.067
<b>1 + 2 → 8</b>	20.43	$4.96 \times 10^{12}$	-7.961
<b>1 + 2 → 9</b>	24.24	$2.75 \times 10^{12}$	-7.530
<b>1 + 2 → 10</b>	18.55	$2.95 \times 10^{10}$	-6.975
<b>1 + 2 → 13</b>	38.41	$2.95 \times 10^{30}$	-12.578
<b>1 + 2 → 20</b>	56.34	$2.61 \times 10^{49}$	-17.784
<b>1 + 2 → 26</b>	36.51	$6.76 \times 10^{28}$	-11.947
<b>1 + 2 → 7 + H</b>	43.67	$1.38 \times 10^8$	-5.345
<b>1 + 2 → 11 + H</b>	38.30	$1.13 \times 10^6$	-4.817
<b>1 + 2 → 18 + 19</b>	65.80	$2.97 \times 10^{50}$	-17.388
<b>1 + 2 → 25 + 19</b>	54.51	$8.15 \times 10^{37}$	-13.800

<sup>a</sup>  $k = A'T^n \exp(-E_a/RT)$ .  $E_a$  in kcal mol<sup>-1</sup>,  $A'T^n$  in cm<sup>3</sup> molecule<sup>-1</sup> s<sup>-1</sup>.

reaction slow at temperatures relevant to, for example, the ISM and Titan (*e.g.*,  $k \approx 10^{-19}$  cm<sup>3</sup> molecule<sup>-1</sup> s<sup>-1</sup> at 300 K). Total rate constants calculated in the  $C_4H_2 + C_3H_3$  reaction for relevant combustion conditions of 10 atm and 600–2000 K are plotted in Fig. 5, with branching ratios to the different product sets shown in Fig. 6. At the low-temperature end of this range, the activated  $[C_7H_5]^*$  adduct is predominantly quenched as the open-chain isomers **3** and **10**. In a sooting flame these radicals should isomerize relatively rapidly to form the fulvenallenyl radical, or react further with unsaturated hydrocarbons in molecular weight growth processes. As temperature increases the activated adduct has sufficient energy to isomerize to fulvenallenyl (**9**) or other  $C_7H_5$  isomers (such as **26** and **20**) before being collisionally deactivated. At around 1500 K and above the activated  $[C_7H_5]^*$  adduct has sufficient energy to dissociate to new products before collisional deactivation. Reverse reaction to  $C_4H_2 + C_3H_3$  is the major  $C_7H_5$  dissociation channel, and as a result the total rate for formation of new products plateaus at  $<10^{-13}$  cm<sup>3</sup> molecule<sup>-1</sup> s<sup>-1</sup> (considerably below the high-pressure limit value). At around 1500 K and above the formation of other dissociated product sets is also significant, especially **25 + 19** but also **11 + H**, **18 + 19**, and **7 + H**.

For comparison, branching ratios to important products in the  $C_4H_2 + C_3H_3$  reaction at 0.01 atm and 100–2000 K are illustrated in Fig. 7. Here we can clearly observe the transition from quenching of the initial association products at low temperatures, to isomerization of the activated  $[C_7H_5]^*$  radical to fulvenallenyl (**9**) at intermediate temperatures, and ultimately dissociation to *i*-C<sub>3</sub>H<sub>3</sub> + C<sub>2</sub>H<sub>2</sub> (**25 + 19**) and other product sets at high temperatures.

Diactylene has been detected at peak mole fractions of around 0.001 to 0.003 in fuel-rich flames of unsaturated hydrocarbons, typically corresponding to around an order of magnitude less than the acetylene concentration,<sup>2</sup> and of similar magnitude to accepted concentrations for propargyl. The reaction of propargyl with diacetylene should proceed with a significant flux relative to the previously considered propargyl + acetylene reaction, given that this latter reaction



**Fig. 5** RRKM/ME rate constants in the  $C_4H_2$  (**1**) +  $C_3H_3$  (**2**) reaction, at 10 atm and 600–2000 K.



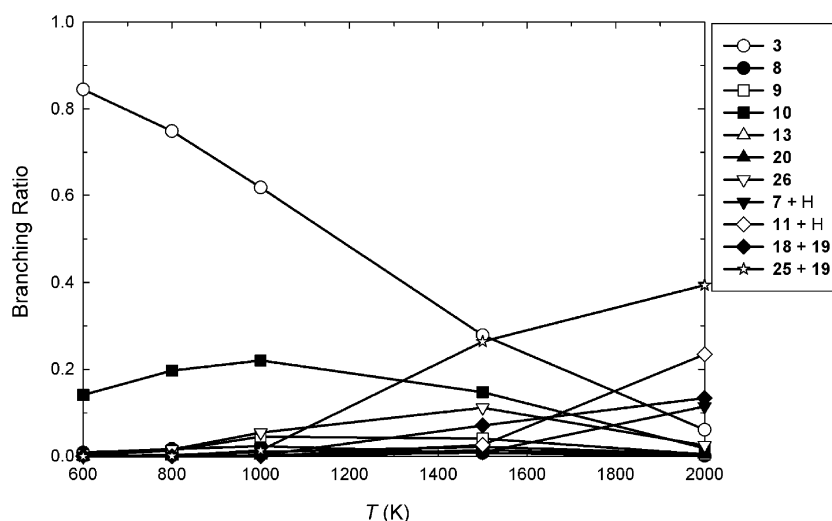


Fig. 6 Branching ratios for new product formation in the  $C_4H_2 + C_3H_3$  reaction, at 10 atm and 600–2000 K.

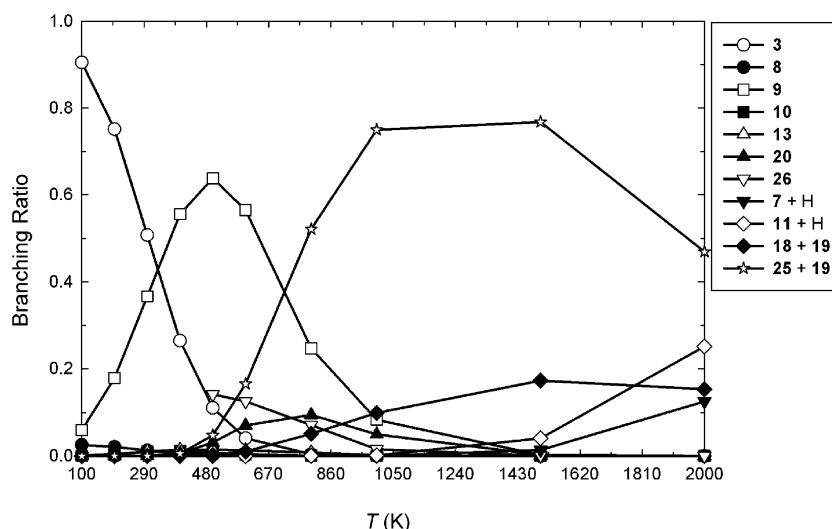


Fig. 7 Branching ratios for new product formation in the  $C_4H_2 + C_3H_3$  reaction, at 0.01 atm and 100–2000 K.

proceeds at a similar (if not slower) rate.<sup>16,17</sup> Indeed, Frenklach<sup>18</sup> has argued that the  $C_3H_3 + C_2H_2$  reaction, with subsequent growth of the *c*- $C_5H_5$  product to benzene, could dominate initial aromatic ring formation under molecular weight growth conditions. The reaction of propargyl and diacetylene is interesting in that it can lead to  $C_7$  products in a single step, bypassing the need for formation of benzene as the first aromatic ring, and within this context it is critical that branching between  $C_5$  and  $C_7$  product sets be accurately characterized as a function of temperature and pressure.

#### *n*- $C_5H_3 + C_2H_2$ reaction kinetics

Calculated rate constants in the two parallel *n*- $C_5H_3 + C_2H_2$  reaction mechanisms at 10 atm and 600–2000 K are shown in Fig. 8, with corresponding branching ratios provided in Fig. 9. Rate constant expressions for important products are provided in Table 2. Fig. 8 demonstrates that the reverse reaction channel to *n*- $C_5H_3 + C_2H_2$  is significant at even moderate temperatures and above (*ca.* 800 K), limiting the

total reaction rate to less than  $10^{-14}$   $\text{cm}^3 \text{molecule}^{-1} \text{s}^{-1}$ . At around 600–1000 K the major products are the  $C_7H_5$  isomers **14** and **16** (the initial reaction adducts), with smaller amounts of **26**, **9**, and **13**. As with the  $C_4H_2 + C_3H_3$  mechanism, further reaction of these  $C_7H_5$  radicals at moderate temperatures is expected to favor formation of the fulvenallenyl radical. At around 1500 K the formation of *i*- $C_5H_3 + C_2H_2$  becomes important, and this process therefore provides a means for isomerization between the *n*- $C_5H_3$  and *i*- $C_5H_3$  isomers. At 2000 K the higher-energy pathways to  $C_7H_4$  species + H increase in significance, with **17** + H now predicted to be the dominant reaction product.

#### *i*- $C_5H_3 + C_2H_2$ reaction kinetics

Rate constants and branching ratios in the *i*- $C_5H_3 + C_2H_2$  reaction process, again at 10 atm and 600–2000 K, are presented in Fig. 10 and 11, with rate constant parameters in Table 3. Results for this reaction system are similar to those obtained with the *n*- $C_5H_3$  isomer. At 1000 K and below

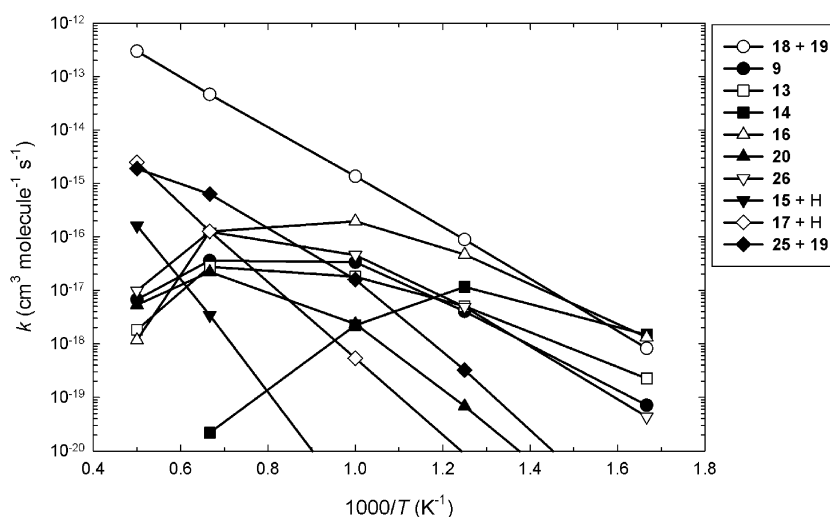


Fig. 8 RRKM/ME rate constants in the  $n\text{-C}_5\text{H}_3 + \text{C}_2\text{H}_2$  reaction, at 10 atm and 600–2000 K.

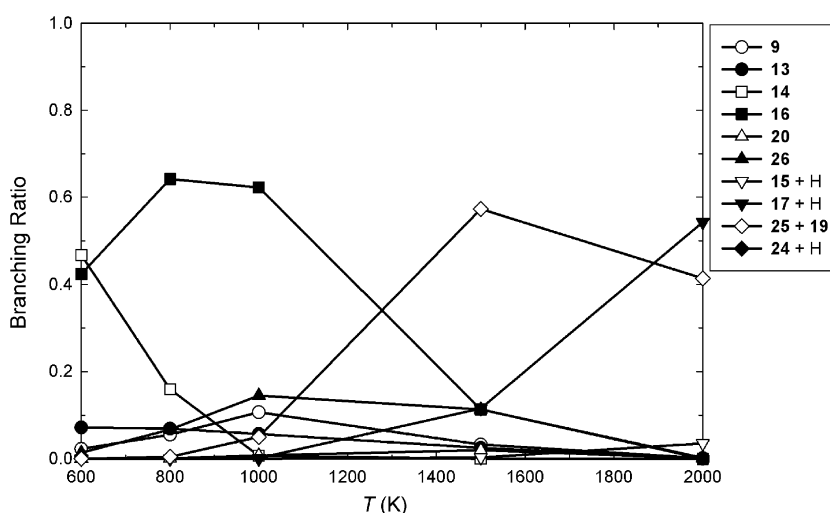


Fig. 9 Branching ratios for new product formation in the  $n\text{-C}_5\text{H}_3 + \text{C}_2\text{H}_2$  reaction, at 10 atm and 600–2000 K.

**Table 2** Rate constant parameters for the formation of important products in the  $i\text{-C}_5\text{H}_3 + \text{C}_2\text{H}_2$  reaction, at 10 atm between 300 and 2000 K<sup>a</sup>

	$E_a$	$A'$	$n$
$25 + 19 \rightarrow 9$	29.54	$1.57 \times 10^{21}$	-10.336
$25 + 19 \rightarrow 13$	42.02	$3.43 \times 10^{40}$	-15.971
$25 + 19 \rightarrow 20$	27.70	$3.37 \times 10^{13}$	-7.769
$25 + 19 \rightarrow 23$	26.22	$5.64 \times 10^{22}$	-11.214
$25 + 19 \rightarrow 26$	30.52	$1.15 \times 10^{29}$	-12.713
$25 + 19 \rightarrow 27$	30.22	$9.25 \times 10^{45}$	-18.414
$25 + 19 \rightarrow 7 + \text{H}$	59.67	$7.37 \times 10^{24}$	-10.040
$25 + 19 \rightarrow 18 + 19$	52.37	$1.38 \times 10^{28}$	-11.231
$25 + 19 \rightarrow 22 + \text{H}$	42.02	$2.80 \times 10^5$	-4.943
$25 + 19 \rightarrow 24 + \text{H}$	54.93	$2.31 \times 10^{24}$	-10.150

<sup>a</sup>  $k = A'T^n \exp(-E_a/RT)$ .  $E_a$  in kcal mol<sup>-1</sup>,  $A'T^n$  in cm<sup>3</sup> molecule<sup>-1</sup> s<sup>-1</sup>.

collisional deactivation of **27** dominates, due to the smaller initial barrier for formation of this radical. The reverse dissociation channel to the reactants **25** + **19** again becomes important at around 800 K and above, with **24** + H and

**7** + H being the most significant new product sets, with formation of  $n\text{-C}_5\text{H}_3 + \text{C}_2\text{H}_2$  being somewhat less important.

#### Further molecular-weight growth chemistry

The results presented here demonstrate that the  $\text{C}_3\text{H}_3 + \text{C}_4\text{H}_2$  reaction (as well as the studied  $\text{C}_5\text{H}_3 + \text{C}_2\text{H}_2$  processes) can produce the fulvenallenyl radical, and other  $\text{C}_7\text{H}_5$  precursors, under conditions relevant to sooting flames. As the fulvenallenyl radical shares properties of propargyl—it can be considered a cyclopentadienyl-substituted propargyl radical—it has the potential to react further with  $\text{C}_4\text{H}_2$  in molecular weight growth processes. Preliminary energy surfaces for the fulvenallenyl radical + diacetylene reaction are provided in Fig. 12 and 13, where the cyclization process reported here for propargyl + diacetylene is considered. These energy surfaces demonstrate that  $\text{C}_4\text{H}_2$  adds to the fulvenallenyl radical with a similar barrier to that required for association with propargyl, producing an activated  $[\text{C}_{11}\text{H}_7]^*$  adduct. Consistent with the analogous  $\text{C}_4\text{H}_2 + \text{C}_3\text{H}_3$  mechanism, this radical can undergo

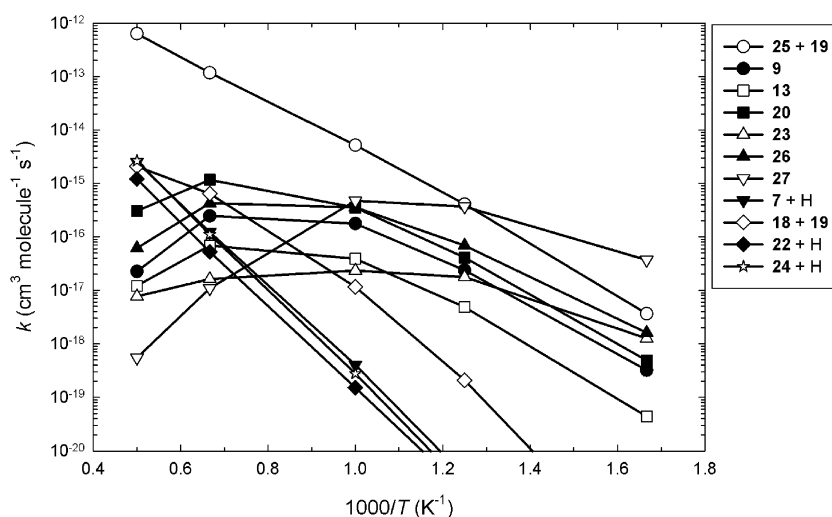


Fig. 10 RRKM/ME rate constants in the  $i\text{-C}_5\text{H}_3 + \text{C}_2\text{H}_2$  reaction, at 10 atm and 600–2000 K.

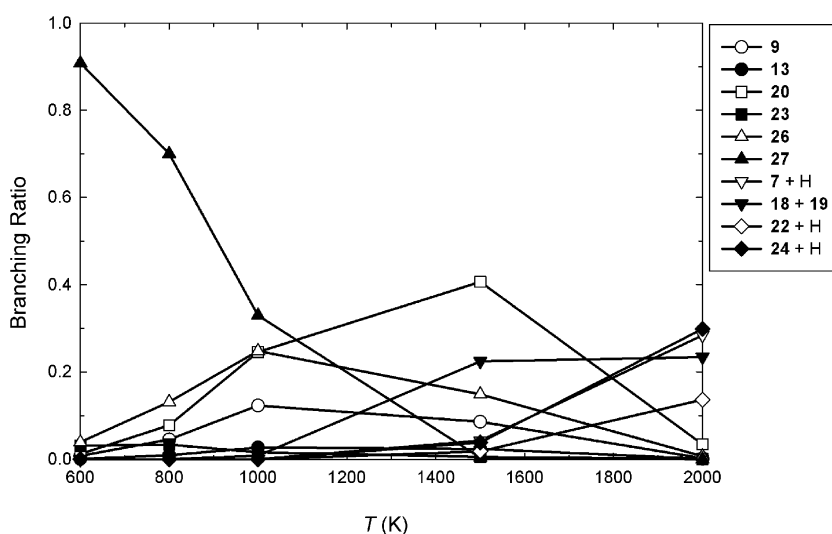


Fig. 11 Branching ratios for new product formation in the  $i\text{-C}_5\text{H}_3 + \text{C}_2\text{H}_2$  reaction, at 10 atm and 600–2000 K.

**Table 3** Rate constant parameters for the formation of important products in the  $n\text{-C}_5\text{H}_3 + \text{C}_2\text{H}_2$  reaction, at 10 atm between 300 and 2000 K<sup>a</sup>

	$E_a$	$A'$	$n$
$18 + 19 \rightarrow 9$	32.77	$1.92 \times 10^{25}$	-11.679
$18 + 19 \rightarrow 13$	31.55	$1.87 \times 10^{28}$	-12.778
$18 + 19 \rightarrow 14$	35.93	$1.14 \times 10^{61}$	-23.676
$18 + 19 \rightarrow 16$	31.71	$1.03 \times 10^{35}$	-14.776
$18 + 19 \rightarrow 20$	60.94	$1.46 \times 10^{57}$	-20.501
$18 + 19 \rightarrow 26$	39.09	$1.94 \times 10^{36}$	-14.793
$18 + 19 \rightarrow 15 + \text{H}$	74.24	$6.93 \times 10^{23}$	-9.569
$18 + 19 \rightarrow 17 + \text{H}$	53.49	$1.06 \times 10^{24}$	-10.069
$18 + 19 \rightarrow 25 + 19$	45.79	$1.85 \times 10^{21}$	-9.380

<sup>a</sup>  $k = A'T^n \exp(-E_a/RT)$ .  $E_a$  in kcal mol<sup>-1</sup>,  $A'T^n$  in cm<sup>3</sup> molecule<sup>-1</sup> s<sup>-1</sup>.

a low-energy ring-closing reaction to a polycyclic radical with two spiro-conjugated five-member rings. Unlike the  $\text{C}_7\text{H}_5$  analog, however, this species does not have a methylene group adjacent to the radical site to facilitate a 1,2-hydrogen shift.

Instead, the radical site can be attacked by a CH moiety from the adjacent  $\text{C}_5$  ring, enlarging this ring to  $\text{C}_6$  in the process. This reaction occurs below the entrance channel energy and is again exothermic. Ultimately, this process forms an acetylene-substituted indenyl radical (1- or 2-ethynindenyl), which is around 100 kcal mol<sup>-1</sup> more stable than fulvenallenyl +  $\text{C}_4\text{H}_2$ . Interestingly, the exothermicity of these fulvenallenyl +  $\text{C}_4\text{H}_2 \rightarrow$  1-/2-ethynindenyl reactions is considerably greater than that of propargyl +  $\text{C}_4\text{H}_2 \rightarrow$  fulvenallenyl (77 kcal mol<sup>-1</sup>), due to the resonance stabilization of these  $\text{C}_{11}\text{H}_7$  radicals. In fact, the two resonantly stabilized  $\text{C}_{11}\text{H}_7$  radicals reported here appear to be unconsidered in previous studies. Significant quantities of some unidentified  $\text{C}_{11}\text{H}_7$  isomer(s) have been detected however, along with the closed-shell  $\text{C}_{11}\text{H}_8$  parent ethynyl-1*H*-indene, in the pyrolysis of toluene.<sup>19</sup> Toluene pyrolysis produces large amounts of fulvenallene through thermal decomposition of the benzyl radical and the  $c\text{-C}_5\text{H}_5 + \text{C}_2\text{H}_2$  reaction, providing a  $\text{C}_7\text{H}_5$  radical precursor.<sup>7</sup>

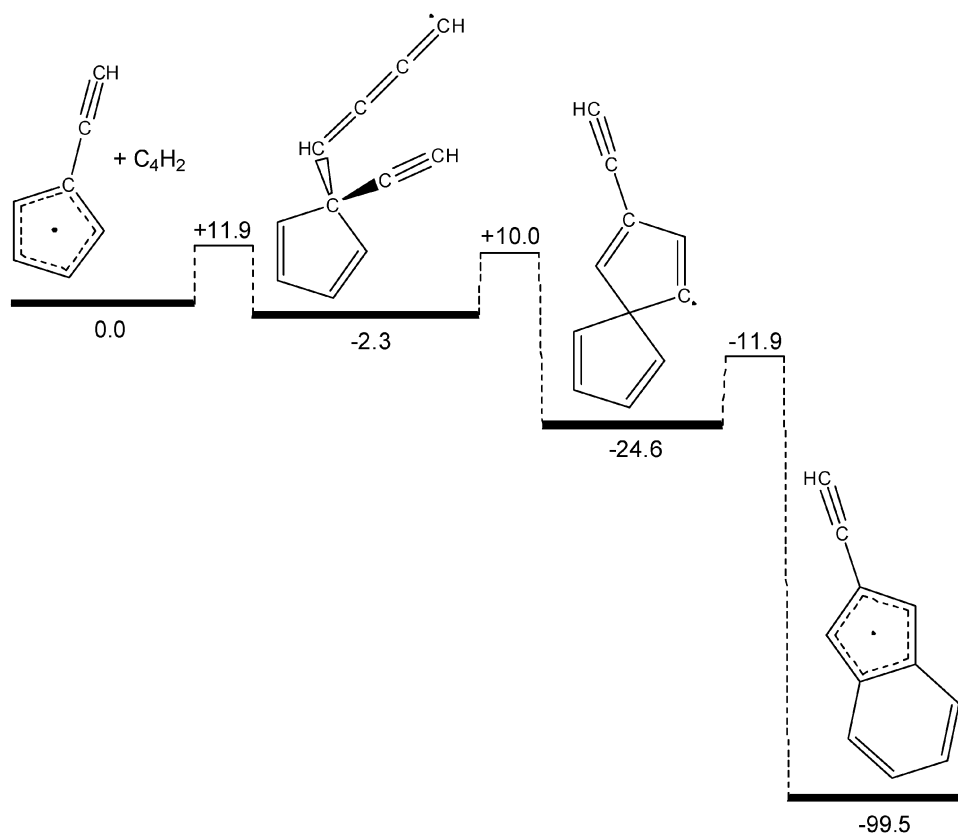


Fig. 12 Energy surface for  $C_4H_2$  addition to the acetylenic form of  $C_7H_5$  (G3SX enthalpies of formation, kcal mol<sup>-1</sup>).

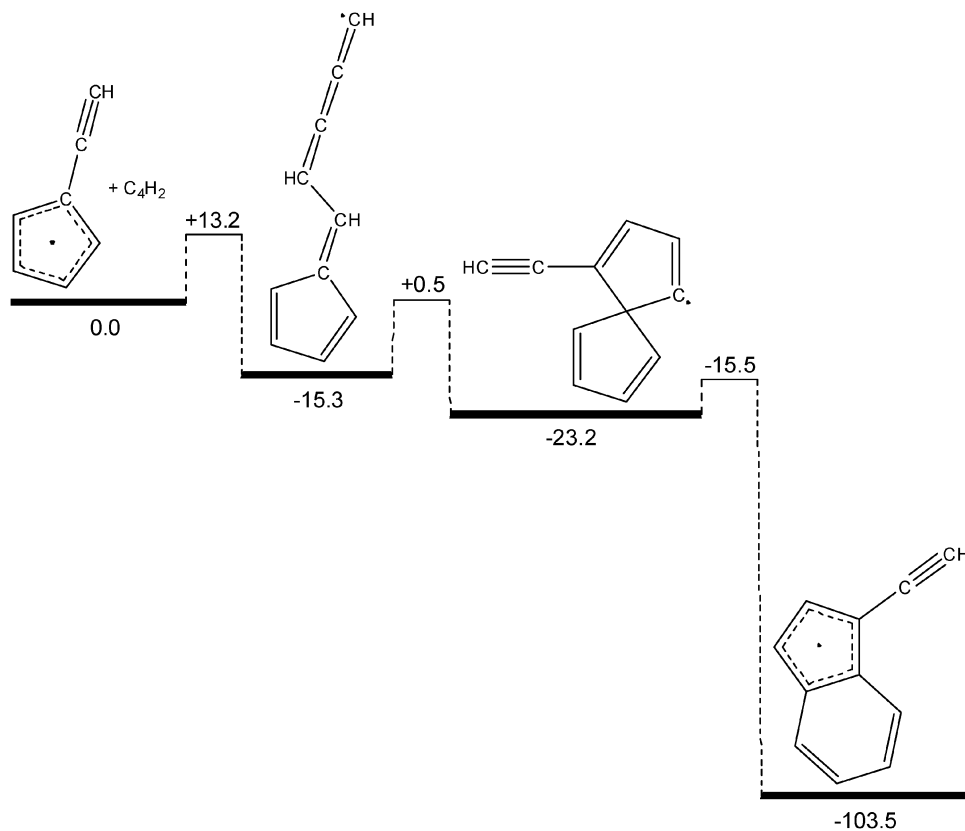
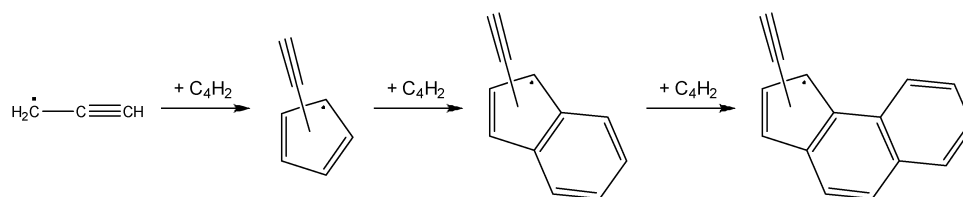


Fig. 13 Energy surface for  $C_4H_2$  addition to the allenic form of  $C_7H_5$  (G3SX enthalpies of formation, kcal mol<sup>-1</sup>).

The  $C_{11}H_7$  ethynindenyl radicals predicted to form in the  $C_7H_5 + C_4H_2$  reaction resemble benzene-fused fulvenallenyl radicals, and this process has therefore achieved the enlargement of the fulvenallenyl radical by one aromatic  $C_6$  ring. These ethynindenyl radicals possess a large number of resonance structures, as the radical electron is delocalized throughout the  $C_5$  and  $C_6$  rings in addition to the acetylene/allene side-chain. This explains the high exothermicity for fulvenallenyl +  $C_4H_2$ , which in turn facilitates CH attack on the radical site in the spiro-conjugated intermediates. The ethynindenyl radicals may be able to undergo further ring growth by addition of a third  $C_4H_2$  unit, as shown below. As such, the  $C_3H_3 + n-C_4H_2$  mechanism is one of the few processes that can initiate ring formation and achieve sustained molecular weight growth. Conventionally, PAH formation is described *via* a mechanism for initial formation of an aromatic ring (*e.g.*, *via* the  $C_3H_3$  self-reaction), followed by a second process for growth of new aromatic units (HACA, *etc.*). When larger polyynes and cyanopolyynes are incorporated into this new chemistry, a variety of ethynyl functionalized and/or *N*-heterocyclic PAHs can be arrived at.



### $C_7H_5$ chemistry

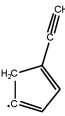
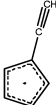
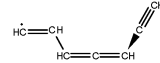
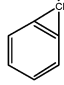
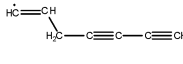

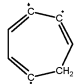
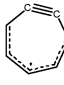

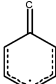
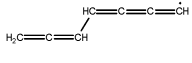
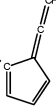
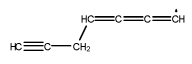
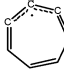
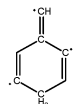
This work provides the most comprehensive evaluation to date of the  $C_7H_5$  energy surface, considering a number of novel isomers and reaction pathways. Table 4 lists in order of their stability ( $G3SX \Delta_f H^{\circ}_0$ ) all  $C_7H_5$  minima identified in this study, along with several isomers reported in previous works.<sup>13</sup> Also included in Table 4 are adiabatic and vertical ionization energies (AIEs and VIEs), which may be useful in differentiating these molecules in tunable VUV photoionization mass spectrometric studies of radical reactions and low-pressure flames. Table 4 reveals that the fulvenallenyl radical ( $\Delta_f H^{\circ}_0 = 115.7 \text{ kcal mol}^{-1}$ ) is the most stable  $C_7H_5$  isomer known, and is likely to be the global minima on the  $C_7H_5$  potential energy surface. Three other  $C_7H_5$  radicals, all resonantly stabilized, have enthalpies of formation 15 to 25  $\text{kcal mol}^{-1}$  larger than fulvenallenyl, whereas the remaining  $C_7H_5$  species are all much less stable. The fulvenallenyl radical should be readily distinguishable from the other resonantly-stabilized  $C_7H_5$  radicals by virtue of its AIE, with the onset of photoionization predicted to occur at photon energies at least 1.5 eV greater than for the other isomers. The fulvenallenyl radical has, in fact, been detected using threshold photoelectron spectroscopy, in a very recent study by Steinbauer *et al.*<sup>20</sup> The fulvenallenyl radical AIE calculated here is similar to the value measured by Steinbauer *et al.* (8.19 eV), and the results in Table 4 support their assignment of the observed  $C_7H_5$  radical as fulvenallenyl.

The new details of  $C_7H_5$  radical chemistry reported in this study may be useful in understanding other important reaction processes involving  $C_7H_5$  reactants, intermediates and products, and some preliminary analysis of these systems is provided here. The fulvenallenyl radical can be produced from the  $C_7H_6$  compounds fulvenallene and 1-ethynylcyclopentadiene *via* low-energy H atom abstraction and C–H bond dissociation reactions.<sup>7</sup> These  $C_7H_6$  compounds, particularly fulvenallene, have been detected at high levels in toluene flames,<sup>21</sup> where they are predicted to arise from thermal decomposition of the benzyl radical.<sup>22,23</sup> Fulvenallene is thought to be a product of the  $c-C_5H_5 + C_2H_2$  reaction,<sup>24</sup> while it may also be produced in xylene oxidation.<sup>10</sup> This work suggests that fulvenallenyl radical decomposition to  $C_4H_2 + C_3H_3$  requires a critical energy of  $85.4 \text{ kcal mol}^{-1}$ , whereas formation of  $n-C_5H_3 + C_2H_2$  and  $i-C_5H_3 + C_2H_2$  requires  $90.6 \text{ kcal mol}^{-1}$  and  $86.7 \text{ kcal mol}^{-1}$ , respectively. Previous kinetic modeling of toluene pyrolysis<sup>25</sup> has estimated that fulvenallenyl radical decomposition reactions to  $C_4H_2 + C_3H_3$  and to a  $C_5H_3$  isomer +  $C_2H_2$  require activation energies of  $62.3 \text{ kcal mol}^{-1}$  in the high-pressure limit, by analogy to  $c-C_5H_5$  radical decomposition. This work indicates

that the fulvenallenyl radical is considerably more stable than presently thought, providing increased opportunity for molecular weight growth reactions, along with a decreased source of the propargyl radical, in toluene pyrolysis and combustion.

From this study it is evident that the title reactions have significant entrance channel barriers. In very low temperature environments ( $< 300 \text{ K}$ ) these reactions are therefore likely to be very slow and this lessens their impact on molecular weight growth schemes. In the Titan atmosphere, where temperatures are in the 70–200 K range, other radical-mediated reaction pathways with barrierless entrance channels will have more rapid kinetics. The  $C_7H_5$  PES is however significant for models of Titan's atmospheric chemistry. For example, the  $C_4H + C_3H_4$  reaction is included in model schemes,<sup>26</sup> where  $C_3H_4$  can be either allene or propyne, and in both cases reaction with the  $C_4H$  radical is suspected to proceed *via* addition to unsaturated carbons forming a  $C_7H_5$  radical intermediate. The subsequent formation of  $C_7H_4$  from H elimination can lead to further radical-mediated growth chemistry, for example the addition reaction  $C_2H + C_7H_4$ .<sup>26</sup> The very low temperature kinetics of  $C_4H$  reactions with allene and propyne have been measured by Sims and coworkers who reveal fast, collision-limited rate constants at Titan-relevant temperatures of 39 K to 300 K;<sup>27,28</sup> this suggests barrierless entrance channels in both cases. These kinetic measurements follow the disappearance of  $C_4H$  radicals and, as such, do not provide any direct details of the reaction products. In the case

**Table 4** Standard enthalpies of formation ( $\Delta_f H^\circ_0$ , kcal mol<sup>-1</sup>), adiabatic ionization energies (AIEs, eV), and vertical ionization energies (VIEs, eV) for some C<sub>7</sub>H<sub>5</sub> isomers<sup>a</sup>

			$\Delta_f H^\circ_0$	154.4				
			AIE	8.25				
			VIE	9.28				
	$\Delta_f H^\circ_0$	115.7	$\Delta_f H^\circ_0$	154.5		$\Delta_f H^\circ_0$	179.9	
	AIE	8.30	AIE	8.34		AIE	8.37	
	VIE	8.35	VIE	9.17		VIE	9.15	
	$\Delta_f H^\circ_0$	133.1	$\Delta_f H^\circ_0$	155.0		$\Delta_f H^\circ_0$	180.2	
	AIE	6.36	AIE	5.99		AIE	8.25	
	VIE	6.53	VIE	7.92		VIE	9.05	
	$\Delta_f H^\circ_0$	136.1	$\Delta_f H^\circ_0$	155.8		$\Delta_f H^\circ_0$	180.5	
	AIE	6.81	AIE	8.35		AIE	7.76	
	VIE	7.02	VIE	9.58		VIE	8.24	
	$\Delta_f H^\circ_0$	138.1	$\Delta_f H^\circ_0$	161.8		$\Delta_f H^\circ_0$	189.3	
	AIE	6.65	AIE	8.43		AIE	8.16	
	VIE	6.76	VIE	9.93		VIE	9.24	
	$\Delta_f H^\circ_0$	150.6	$\Delta_f H^\circ_0$	169.5		$\Delta_f H^\circ_0$	189.4	
	AIE	7.45	AIE	7.65		AIE	5.99	
	VIE	7.52	VIE	7.70		VIE	8.75	
	$\Delta_f H^\circ_0$	151.7	$\Delta_f H^\circ_0$	174.0		$\Delta_f H^\circ_0$	207.6	
	AIE	8.39	AIE	7.82		AIE	5.96	
	VIE	9.50	VIE	7.86		VIE	7.89	
	$\Delta_f H^\circ_0$	153.5	$\Delta_f H^\circ_0$	178.1		$\Delta_f H^\circ_0$	218.6	
	AIE	5.48	AIE	4.41		AIE	5.36	
	VIE	7.41	VIE	9.61		VIE	7.70	

<sup>a</sup> G3SX level of theory.

of C<sub>4</sub>H + propyne, these authors suggest that hydrogen displacement channels are likely, leading to linear C<sub>7</sub>H<sub>4</sub> molecules, with CH<sub>3</sub> elimination channels leading to triacetylene (C<sub>6</sub>H<sub>2</sub>) also possible. For C<sub>4</sub>H + allene, similar H and CH<sub>3</sub> elimination channels are both possible. At the G3SX level of theory the C<sub>4</sub>H + propyne 0 K heat of formation is 234.4 kcal mol<sup>-1</sup>, while for C<sub>4</sub>H + allene it is 235.3 kcal mol<sup>-1</sup>. This indicates that the initial adducts formed in both reactions will be provided with sufficient energy to access all reaction channels identified in this study, although whether or not these adducts can isomerize onto the energy surface developed here is not yet apparent. Several of the linear C<sub>7</sub>H<sub>4</sub> isomers presently included in models of Titan's atmosphere, formed in the C<sub>4</sub>H + C<sub>3</sub>H<sub>4</sub> reactions or otherwise, are shown here to rapidly react with H, forming activated adducts that may react further to form product sets including cyclic C<sub>7</sub>H<sub>5</sub> species, C<sub>5</sub>H<sub>3</sub> radicals + acetylene, or propargyl + diacetylene. Another potentially important reaction on the C<sub>7</sub>H<sub>5</sub> energy surface is that of *ortho*-benzynes (*c*-C<sub>6</sub>H<sub>4</sub>) with the methylidyne (CH) radical. At the G3SX level, the benzyne + CH heat of

formation is 253.4 kcal mol<sup>-1</sup> (0 K), considerably above that of the C<sub>4</sub>H<sub>2</sub> + C<sub>3</sub>H<sub>3</sub>, C<sub>5</sub>H<sub>3</sub> + C<sub>2</sub>H<sub>2</sub>, and C<sub>7</sub>H<sub>4</sub> + H product sets. Reactions of the CH radical are also considered to be important to the chemistry of Titan, and generally proceed with negligible activation energy.<sup>29</sup> The low pressures encountered in the atmosphere of Titan and in the ISM mean that the highly activated [C<sub>7</sub>H<sub>5</sub>]\* adduct formed in this reaction would likely have sufficient energy to dissociate to a number of different product sets in a direct, chemically activated process even at relatively low temperatures.

The formation of a C<sub>7</sub>H<sub>5</sub> radical product (+H) has been previously considered in the benzene + C(<sup>3</sup>P) reaction, which is of astrochemical importance. This reaction proceeds on a C<sub>7</sub>H<sub>6</sub> energy surface, and is thought to form collisionally deactivated C<sub>7</sub>H<sub>6</sub> and dissociated C<sub>7</sub>H<sub>5</sub> + H product sets, although their structures remain unconfirmed.<sup>13</sup> The benzene + C(<sup>3</sup>P) reactants have an enthalpy of formation of 194.6 kcal mol<sup>-1</sup> (0 K, G3SX), making production of previously-considered C<sub>7</sub>H<sub>5</sub> radicals + H, like the seven-member ring **5**, only mildly exothermic. The fulvenallenyl

radical has not been considered as a product of the benzene + C(<sup>3</sup>P) reaction, although if favorable reaction pathways are available it could be produced at around 25 kcal mol<sup>-1</sup> below the entrance channel energy. Kaiser *et al.*<sup>13a</sup> have shown how the benzene + C reaction can lead to phenylcarbene without a barrier, *via* insertion into a C–C bond followed by low-energy ring closing/opening steps. It is known that phenylcarbene rearranges to fulvenallene,<sup>30</sup> which would then have sufficient energy to dissociate to fulvenallenyl + H.

## Conclusions

This study presents a comprehensive C<sub>7</sub>H<sub>5</sub> energy surface, which is used in master equation simulations to study the reaction of propargyl (C<sub>3</sub>H<sub>3</sub>) with diacetylene (C<sub>4</sub>H<sub>2</sub>), as well as the reaction of the *i*-C<sub>5</sub>H<sub>3</sub> and *n*-C<sub>5</sub>H<sub>3</sub> isomers with acetylene (C<sub>2</sub>H<sub>2</sub>). Addition of propargyl to diacetylene requires a moderate barrier, but forms an activated C<sub>7</sub>H<sub>5</sub> adduct with sufficient energy to isomerize to the fulvenallenyl radical. At high temperatures formation of the C<sub>5</sub>H<sub>3</sub> isomers + C<sub>2</sub>H<sub>2</sub>, as well as a number of C<sub>7</sub>H<sub>4</sub> isomers + H becomes important. Further PAH molecular growth reactions of the fulvenallenyl radical, involving repeated C<sub>3</sub>H<sub>3</sub> addition, are proposed. Other important reactions involving the C<sub>7</sub>H<sub>5</sub> energy surface are also discussed, in light of the new details about C<sub>7</sub>H<sub>5</sub> chemistry reported here.

## Acknowledgements

A.J.T acknowledges funding through the Australian Research Council (DP1094135). G.d.S. is grateful to the Victorian Partnership for Advanced Computing (VPAC) for providing computational resources.

## References

- J. Cernicharo, A. M. Heras, A. G. G. M. Tielens, J. R. Pardo, F. Herpin, M. Guélin and L. B. F. M. Waters, *Astrophys. J.*, 2001, **546**, L123.
- N. Hansen, S. J. Klippenstein, P. R. Westmoreland, T. Kasper, K. Kohse-Hoinghaus, J. Wang and T. A. Cool, *Phys. Chem. Chem. Phys.*, 2008, **10**, 366.
- Y. Li, L. Zhang, Z. Tian, T. Yuan, K. Zhang, B. Yang and F. Qi, *Proc. Combust. Inst.*, 2009, **32**, 1293.
- E. Hebrard, M. Dobrijevic, Y. Benilan and F. Raulin, *J. Photochem. Photobiol., C*, 2006, **7**, 211.
- A. Indarto, A. Giordana, G. Ghigo and G. Tonachini, *J. Phys. Org. Chem.*, 2010, **23**, 400.
- A. V. Krestinin, *Combust. Flame*, 2000, **121**, 513.
- G. da Silva and J. W. Bozzelli, *J. Phys. Chem. A*, 2009, **113**, 12045.
- L. A. Curtiss, P. C. Redfern, K. Raghavachari and J. A. Pople, *J. Chem. Phys.*, 2001, **114**, 108.
- J. Zheng, Y. Zhao and D. G. Truhlar, *J. Chem. Theory. Comput.*, 2009, **5**, 808.
- G. da Silva, E. E. Moore and J. W. Bozzelli, *J. Phys. Chem. A*, 2009, **113**, 10264.
- M. J. Frisch, G. W. Trucks, H. B. Schlegel, G. E. Scuseria, M. A. Robb, J. R. Cheeseman, G. Scalmani, V. Barone, B. Mennucci, G. A. Petersson, H. Nakatsuji, M. Caricato, X. Li, H. P. Hratchian, A. F. Izmaylov, J. Bloino, G. Zheng, J. L. Sonnenberg, M. Hada, M. Ehara, K. Toyota, R. Fukuda, J. Hasegawa, M. Ishida, T. Nakajima, Y. Honda, O. Kitao, H. Nakai, T. Vreven, J. A. Montgomery, Jr., J. E. Peralta, F. Ogliaro, M. Bearpark, J. J. Heyd, E. Brothers, K. N. Kudin, V. N. Staroverov, R. Kobayashi, J. Normand, K. Raghavachari, A. Rendell, J. C. Burant, S. S. Iyengar, J. Tomasi, M. Cossi, N. Rega, J. M. Millam, M. Klene, J. E. Knox, J. B. Cross, V. Bakken, C. Adamo, J. Jaramillo, R. Gomperts, R. E. Stratmann, O. Yazyev, A. J. Austin, R. Cammi, C. Pomelli, J. W. Ochterski, R. L. Martin, K. Morokuma, V. G. Zakrzewski, G. A. Voth, P. Salvador, J. J. Dannenberg, S. Dapprich, A. D. Daniels, Ö. Farkas, J. B. Foresman, J. V. Ortiz, J. Cioslowski and D. J. Fox, *Gaussian 09, revision A.02*, Gaussian, Inc., Wallingford, CT, 2009.
- (a) MultiWell-2010.1 Software, 2010, designed and maintained by J. R. Barker with contributors N. F. Ortiz, J. M. Preses, L. L. Lohr, A. Maranzana, P. J. Stimac, T. Lam Nguyen and T. J. Dhilip Kumar; University of Michigan, Ann Arbor, MI; <http://aoss.engin.umich.edu/multiwell/>; (b) J. R. Barker, *Int. J. Chem. Kinet.*, 2001, **33**, 232; (c) J. R. Barker, *Int. J. Chem. Kinet.*, 2009, **41**, 748; (d) T. L. Nguyen and J. R. Barker, *J. Phys. Chem. A*, 2010, **114**, 3718.
- (a) R. I. Kaiser, I. Hahndorf, L. C. L. Huang, Y. T. Lee, H. F. Bettinger, P. v. R. Schleyer, H. F. Schaefer, III and P. R. Schreiner, *J. Chem. Phys.*, 1999, **110**, 6091; (b) H. F. Bettinger, P. v. R. Schleyer, H. F. Schaefer, III, P. R. Schreiner, R. I. Kaiser and Y. T. Lee, *J. Chem. Phys.*, 2000, **113**, 4250; (c) I. Hahndorf, Y. T. Lee, R. I. Kaiser, L. Vereecken, J. Peeters, H. F. Bettinger, P. R. Schreiner, P. v. R. Schleyer, W. D. Allen and H. F. Schaefer, III, *J. Chem. Phys.*, 2002, **116**, 3248; (d) R. I. Kaiser, L. Vereecken, J. Peeters, H. F. Bettinger, P. v. R. Schleyer and H. F. Schaefer, III, *Astron. Astrophys.*, 2003, **406**, 385.
- (a) S. Fascella, C. Cavallotti, R. Rota and S. Carra, *J. Phys. Chem. A*, 2005, **109**, 7546; (b) C. Cavallotti, M. Derudi and R. Rota, *Proc. Combust. Inst.*, 2009, **32**, 115.
- N. Hansen, S. J. Klippenstein, J. A. Miller, J. Wang, T. A. Cool, M. E. Law, P. R. Westmoreland, T. Kasper and K. Kohse-Hoinghaus, *J. Phys. Chem. A*, 2006, **110**, 4376.
- L. V. Moskaleva and M. C. Lin, *J. Comput. Chem.*, 2000, **21**, 415.
- V. D. Knyazev and I. R. Slagle, *J. Phys. Chem. A*, 2002, **106**, 5613.
- M. Frenklach, *Phys. Chem. Chem. Phys.*, 2002, **4**, 2028.
- T. Zhang, L. Zhang, X. Hong, K. Zhang, F. Qi, C. K. Law, T. Ye, P. Zhao and Y. Chen, *Combust. Flame*, 2009, **156**, 2071.
- M. Steinbauer, P. Hemberger, I. Fischer and A. Bodi, *ChemPhysChem*, 2010, DOI: 10.1002/cphc.201000892.
- Y. Li, L. Zhang, Z. Tian, T. Yuan, J. Wang, B. Yang and F. Qi, *Energy Fuels*, 2009, **23**, 1473.
- G. da Silva, J. A. Cole and J. W. Bozzelli, *J. Phys. Chem. A*, 2009, **113**, 6111.
- C. Cavallotti, M. Derudi and R. Rota, *Proc. Combust. Inst.*, 2009, **32**, 115.
- G. da Silva, J. A. Cole and J. W. Bozzelli, *J. Phys. Chem. A*, 2010, **114**, 2275.
- L. Zhang, J. Cai, T. Zhang and F. Qi, *Combust. Flame*, 2010, **157**, 1686.
- V. A. Krasnopolsky, *Icarus*, 2009, **201**, 226.
- C. Berteloite, S. D. Le Picard, N. Balucani, A. Canosa and I. R. Sims, *Phys. Chem. Chem. Phys.*, 2010, **12**, 3677.
- C. Berteloite, S. D. Le Picard, P. Birza, M. C. Gazeau, A. Canosa, Y. Benilan and I. R. Sims, *Icarus*, 2008, **194**, 746.
- F. Goulay, A. J. Trevitt, G. Meloni, T. M. Selby, D. L. Osborn, C. A. Taatjes, L. Vereecken and S. R. Leone, *J. Am. Chem. Soc.*, 2009, **131**, 993.
- P. Schissel, M. E. Kent, D. J. McAdoo and E. Hedaya, *J. Am. Chem. Soc.*, 1970, **92**, 2147.